

14th Hypervelocity Impact Symposium 2017, HVIS2017, 24-28 April 2017, Canterbury, Kent,  
UK

## Modeling impact outcomes for the Double Asteroid Redirection Test (DART) mission

A.M. Stickle<sup>a\*</sup>, E.S.G. Rainey<sup>a</sup>, M. Bruck Syal<sup>b</sup>, J.M. Owen<sup>b</sup>, P. Miller<sup>b</sup>, O.S. Barnouin<sup>a</sup>,  
C.M. Ernst<sup>a</sup>, and the AIDA Impact Simulation Working Group\*

<sup>a</sup>Johns Hopkins University Applied Physics Laboratory, 11100 Johns Hopkins Rd. M/S 200-W230, Laurel, MD 20723, USA

<sup>b</sup>Lawrence Livermore National Laboratory, Livermore CA, USA

---

### Abstract

The Double Asteroid Redirection Test (DART) is a NASA mission concept currently in Phase-A study, which will provide the first full-scale test of a kinetic impactor deflection mission for planetary defense. The DART spacecraft will target the moon of Didymos (Didymos-B, or “Didymoon”) and impact the smaller body at ~6 km/s with ~500 kg mass. The change in orbital period of the moon will then be measured using ground-based observations, which can be used to estimate the momentum enhancement of the moon from the impact. Impact modeling provides a basis for interpretation of the DART impact and observations (including the calculation of the momentum enhancement,  $\beta$ , the period change, and ejecta mass for a given impact scenario). Here, we present results from simulations using the shock physics codes CTH and Spheral of a DART-like impact into an asteroid target. Variations in target composition and porosity are simulated to examine their effect on  $\beta$ . A variety of methods are used to calculate  $\beta$ , and these simulations suggest that  $\beta$  can be calculated using any of them, depending on what type of simulation is performed, and provide consistent results. The results also indicate that varying the target composition (e.g., whether the target is made up of something granite-like or more akin to basalt or pumice) does not significantly affect the results. More significant changes are seen when parameters such as porosity are varied: increased porosity decreases  $\beta$ , alters the crater shape, and increases  $\Delta v$ . Simulations also suggest that the form of porosity is important: macro-porosity has a significant effect on the cratering process that is different than equivalent micro-porosity.

© 2017 The Authors. Published by Elsevier Ltd.

Peer-review under responsibility of the scientific committee of the 14th Hypervelocity Impact Symposium 2017.

**Keywords:** Planetary Impact; Momentum Enhancement; Hydrocodes; CTH; Spheral; DART Mission

---

---

\* Corresponding author. Tel.: +1-240-228-3822; fax: +1-240-228-8939.

E-mail address: [Angela.Stickle@jhuapl.edu](mailto:Angela.Stickle@jhuapl.edu)

## 1. Introduction

### Nomenclature

$\beta$	momentum enhancement factor
$p_{s/c}$	momentum of the incoming spacecraft
$p_{ejecta}$	component of the escaping ejecta momentum lying along the direction of the impact trajectory
$\Delta v$	change in velocity of the target (“Didymoon”) following the DART impact

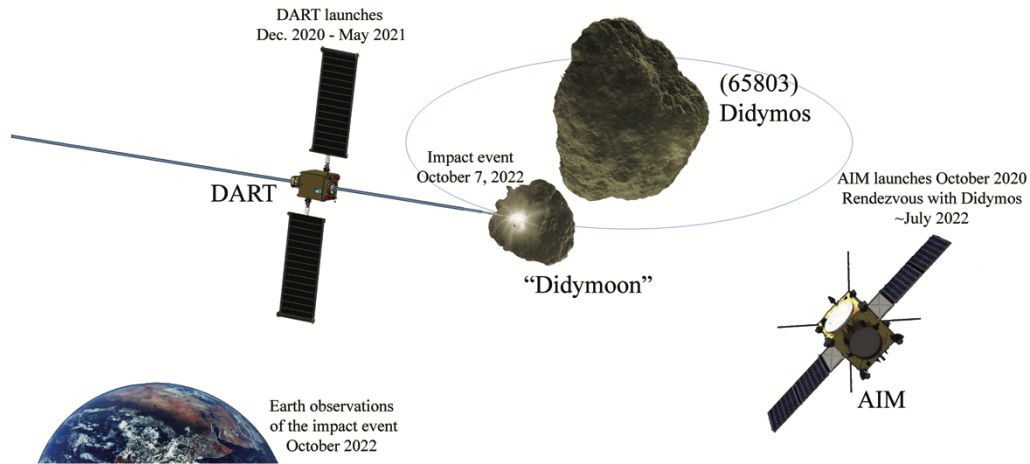


Figure 1. Schematic of the Double Asteroid Redirection Test. The DART mission utilizes NASA’s Evolutionary Xenon Thruster (NEXT-C) engines, which provides flexibility in the launch window timing while still maintaining an October 2022 impact at the Didymos system.

### 1.1. The Double Asteroid Redirection Test

The Double Asteroid Redirection Test (DART) is a NASA mission concept currently in Phase-A study [1]. DART will provide the first full-scale test of a kinetic impactor deflection mission for planetary defense. The mission will launch in late 2020 or early 2021 and impact its target in October 2022 (Figure 1). The target of the DART mission is the 65803 Didymos system, which is a binary asteroid system that makes an unusually close approach to the Earth in 2022 and 2024. These close approaches make it an ideal target for a kinetic impact deflection experiment mission, as the expected deflection can be observed from the Earth. The DART spacecraft will target the moon of Didymos (Didymos-B, or “Didymoon”) and impact the smaller body at ~6 km/s with ~500 kg mass. The change in orbital period of the moon will then be measured using ground-based observations. Measuring the change in period will allow the momentum enhancement of the moon to be estimated using the momentum enhancement factor,  $\beta$ :

$$\beta = 1 + \frac{p_{moon}}{p_{spacecraft}} \quad (1)$$

where the momentum of the moon,  $p_{moon} = \text{mass}_{moon} * \Delta v_{moon}$  and the mass of the moon is estimated from size of Didymos-B and assumed material properties,  $\Delta v_{moon}$  is determined from the period change, and the incoming momentum of the spacecraft is known.

A companion European Space Agency mission is also under consideration with ESA, called the Asteroid Impact Mission (AIM). The purpose of AIM is to scout the Didymos system prior to DART’s arrival, be present

during the impact, and provide post-impact information about the changes within the system (including crater size, ejecta amount, period change). A primary measurement that AIM could make is the mass of the moon of Didymos, which is helpful in calculating the momentum transfer to the body directly. An ideal flight scenario for AIM will rendezvous with the Didymos system in the summer of 2022, which provides overlap with the DART mission impact (Figure 1).

### *1.2. Modeling the DART Impact*

While testing kinetic impactor technology, another primary objective of the DART mission is to improve and validate impact models to provide confidence in extrapolation to other deflection scenarios. DART will join LCROSS and Deep Impact as one of three full-scale impact experiments, and is the only case where we expect to be able to measure the resulting deflection of the target. Though they remain the dominant method of using laboratory insights to understand large-scale structures, scaling laws (e.g., [2]) require knowledge of target and projectile properties (e.g., strength). Imagery returned from the spacecraft prior to impact will allow some characterization of the impact site, though many of the target properties remain unknown. Numerical and analytical models provide a means to better constrain these properties. In support of the mission concept, modeling studies were performed to better understand the expected period change of the small moon, the momentum enhancement of the body from the impactor, as well as the relationship between these observables and material properties of the asteroid.

Impact modeling provides a basis for interpretation of the DART impact and observations (including the calculation of the momentum enhancement,  $\beta$ , the period change, and ejecta mass for a given impact scenario). Part of the study being performed for the DART mission includes a suite of impact models to better understand the likely outcomes of the impact. The Didymos system is composed of a primary body (diameter ~800 m) and companion (“Didymoon”, diameter ~170 m). A range of target properties is examined to provide best estimates for the impact results, and to investigate how  $\beta$  varies with target/impactor properties, impact conditions, and calculation setup. We use the CTH hydrocode [3] developed by Sandia National Laboratories and the Spheral code developed by Lawrence Livermore National Laboratory [4,5] to model a variety of impact scenarios. Here, we describe preliminary studies testing the effectiveness of the kinetic impactor to deflect a Didymoon-like target with a variety of possible compositions and material properties.

## **2. Methods**

### *2.1. Impact Simulations*

The possible parameter space for the DART impact is large, including variations in material strength, porosity, topography, and composition. This large of a problem lends itself to a relatively large team of impact modelers to best address the various possible impact conditions. Because of this, multiple impact codes are used to sample portions of the parameter space. A separate benchmarking campaign [6] is being undertaken as part of the DART mission studies to ensure that the results of these separate codes can be fully integrated and understood in context. Here, we present simulations results from two codes: CTH and Spheral. Because the size of the spacecraft (~2 m) is small with respect to the target moon (~150 m), these simulations treated the target asteroid as a half-space.

CTH is a two-step Eulerian shock physics hydrocode [3]. The code has the ability to consider multiple materials and rheologies using a wide variety of material models and equations of state (EOS). Both large-scale and small-scale simulations are examined. Adaptive Mesh Refinement (AMR) [7] allows for high resolution over the areas of interest while maintaining reasonable computational time. Here, refinement is focused on moving material interfaces to track ejecta particles. Simulations were performed in a variety geometries: Full-scale DART-representative impacts (32-cm aluminum sphere into a 160-m basaltic sphere), 0.635-cm aluminum or basaltic spheres into a basaltic half-space at 6 km/s, and 0.635-cm aluminum sphere into a 20-cm basaltic sphere at 5-6 km/s. All impacts are at 90° in a 3D rectangular coordinate space. Laboratory-scale simulations were also performed to examine the effects of porosity over a wider range, with values of  $\phi=0, 20, 45$ , and 60% examined for a 0.635-cm basalt sphere impacting into a basalt half space at 5 km/s. The strength of the basaltic targets and projectile were represented using a pressure-dependent yield surface coupled to a Johnson-Cook fracture model to track subsurface damage [8], as

well as a Tillotson EOS with parameters from [9] and a  $p$ - $\alpha$  porosity model using a crush curve for pumice from [10]. Aluminum projectiles were represented using a Johnson-Cook plasticity model and a Tillotson EOS [9].

It is unlikely that the target moon will be a coherent, intact block of material. Theories for binary formation suggest that it is likely that the moon in the system will, instead, be a “rubble pile” and made up of many smaller fragments gravitationally bound together. These might suggest significant *macroporosity* in the target. To test what effects this might have on the momentum transfer, preliminary calculations were performed comparing intact material to two separate porous targets: one with  $\sim 20\%$  microporosity and one with  $\sim 20\%$  macroporosity. Here, the strength of the material is represented using the “BDL” model in CTH, which is described in [11,12]. The projectile is represented by a 60-cm aluminum sphere. A SESAME EOS is used for both target (basalt) and projectile (aluminum) material. Microporosity is simulated using a  $p$ - $\alpha$  model. To generate the macroporosity, a multi-step process was used. The initial particle geometries and packing configuration were generated using the ParticlePack code (v 3.0), which was developed by Lawrence Livermore National Laboratory [13]. This code can generate 2D or 3D particles enclosed in a variety of geometries, with a user-defined size-frequency-distribution (*sfd*) and packing level (e.g., pressed or soft-packed). Here, the particle *sfd* was chosen to provide  $\sim 20\%$  porosity in the final target to match the micro-porosity case. This output was used to generate a CTH input deck with the correct geometry for material particles, and material numbers were randomly assigned to each particle. Here, 2D circular particles were put into a rectangular box in order to perform 2D axisymmetric calculations using CTH.

Spheral is an adaptive Smooth Particle Hydrodynamics (SPH) code being developed at Lawrence Livermore National Laboratories. SPH is a type of meshless computational scheme that is well-suited to track ejecta while avoiding mesh entanglement issues. Adaptive SPH (ASPH) is an extension of typical SPH methods [4]. ASPH allows the smoothing scale to vary with direction, so that anisotropic displacements can be captured more accurately. ASPH results presented here are calculated using the open source code Spheral, which employs an exactly energy preserving method designed to capture adiabatic flow and strong shocks [5]. The damage model employs a statistical representation of flaw- activation strains [14–15, 9]. Spheral includes a tensor form of the damage variable, allowing the directionality of damage to be calculated at each node and thus the tracking of deformation mode [16]. For porous materials the strain- $\alpha$  model of [17] is used. To examine compositional effects, density and strength of the material remained constant between runs, set at:  $\rho = 2.16 \text{ g/cm}^3$  and  $Y_0 = 1 \text{ MPa}$ , respectively. Porosity and Weibull parameters [18–19] varied with material (Table 1).

## 2.2. Calculating Momentum Enhancement

The main parameter of interest resulting from these simulations is the momentum enhancement factor,  $\beta$  (Equation 1). There are two main methods for calculating the momentum of the target following impact: determining the ejecta momentum or calculating the velocity of the target post impact. In the first scenario, ejecta from the impact acts as a thruster on the body. Momentum conservation ensures that the momentum of the ejecta normal to the plane of impact will be balanced by an additional momentum to the target. The momentum of the ejecta, therefore, can be calculated in the numerical simulations and used to calculate  $\beta$  using a modified equation (1) with  $p_{\text{ejecta}}$  replacing  $p_{\text{moon}}$ . The momentum of the ejecta can be measured by tracking specific particles (using Spheral), by tracking mass moving through the grid (CTH), by tagging material using tracer particles and tracking the particle motion (CTH), or by tracking material mass and velocity as it passes a specific plane in the simulation (CTH). The first is the main method for tracking ejecta particles using Spheral, and is used for some calculations using CTH (Section 3.1). Tracking ejecta particles in continuum codes can sometimes present numerical challenges, however, as individual fragments are often not easily tracked or resolved. To avoid this, the velocity change of “Didymoon” following impact can also be measured using tracer particles in the simulations. The mass of the target is known and it is assumed to have zero velocity at the beginning of the simulation, therefore all resulting velocity in the direction of interest following the impact is due to the impact itself, and the momentum can be calculated. For details of this method, see Stickle et al. [20].

To test methods of  $\beta$  calculation (Section 3.1), 2D simulations of a 0.635-cm basalt sphere impacting into a 30-cm basalt sphere at 5 km/s were examined. Basalt was represented using a SESAME EOS, a pressure-dependent plasticity model and a Johnson-Cook fracture model to track damage evolution. Tracers were embedded in every cell within the grid in bands across the target (Figure 2a), and the simulations had a maximum resolution of 0.01 cm (3 cppr).

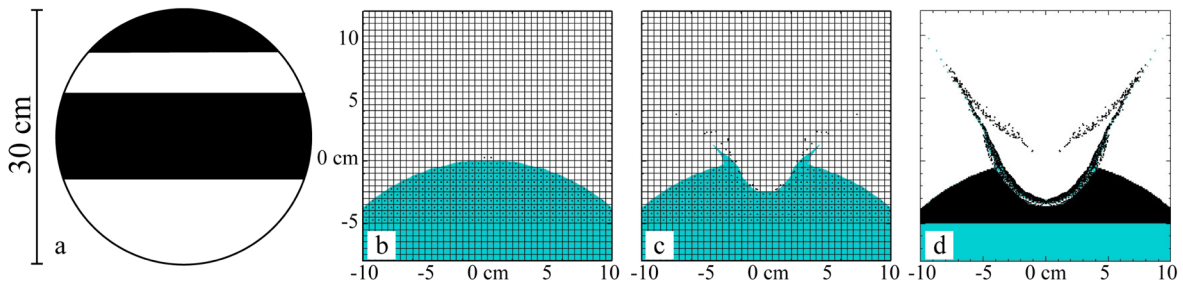


Figure 2. Setup and simulation results for testing beta calculation schemes. a) schematic showing the spherical target with location of defined bands of tracers. b) Setup for calculation, showing a tracer in each grid near the impact point. The simulations were run at a resolution of 0.01-cm, but this image shows a comparable simulation at 0.05-cm resolution for clarity. c) Simulation results 1 msec after impact, showing crater formation and tracer movement tracking ejecta. This simulation is at 0.05-cm resolution, which is shown for clarity. However, the calculations were performed for simulations run at 0.01-cm resolution, which is shown in (d). The higher resolution allows many more tracers to more closely track the material motion.

### 3. Results and Discussion

#### 3.1. Testing methods for calculating momentum enhancement

There are multiple methods to calculate the momentum enhancement factor,  $\beta$ , using impact simulations. Because many different types of codes are being utilized to study the likely output of the DART impact, multiple methods of calculating beta may be used. Here, we calculate  $\beta$  for CTH simulations of an impact into a sphere using three different methods described above to test the repeatability/robustness of the calculations. Method 1 utilized a grid of tracers embedded in a band across the center of the target (Figure 2a), with one tracer in each grid cell. The velocity of these tracers was tracked throughout the simulation and the median vertical velocity at the end of the simulation was used to measure target deflection. Equation (1) was used to calculate  $\beta$ . Method 2 utilized a grid of tracers embedded in a band across the crater zone to track ejecta motion (Figure 2). One tracer was embedded in each cell. The mass and velocity associated with each tracer was calculated as it first passed a plane just above the target and the modified Equation (1) (with  $p_{\text{ejecta}}$  replacing  $p_{\text{moon}}$ ) was used to calculate  $\beta$ . Method 3 tracked all ejecta mass within the grid. Ejecta was defined as mass above the plane of impact with positive vertical velocity and volume fraction within the cell  $< 1$  (i.e., it was a fragment). Equation (1) with  $p_{\text{ejecta}}$  replacing  $p_{\text{moon}}$  was again used to calculate  $\beta$ . Overall, these calculations show that the three different methods of calculating  $\beta$  are consistent with one another. The momentum enhancement factor was calculated as  $\beta=7.79$ ,  $\beta=7.78$ , and  $\beta=7.55$  for methods 1, 2, and 3, respectively. The slightly lower value of  $\beta$  (~3% difference) calculated using method 3 is likely due to some material leaving the grid that is not tracked.

#### 3.2. Effects of target properties on momentum enhancement

The composition and material properties of the moon of Didymos are unknown. Spectral observations of the binary system suggest that the primary body is a “S-type” asteroid, which is the most common compositional group of Near Earth Objects (NEOs). However, the moon of Didymos is too small to be resolved separately from the system, and its composition and properties are unknown. To better bracket possible outcomes of the DART impact, then, impacts into bodies with a variety of compositions and properties are examined to determine the sensitivity of  $\beta$ . Here, the effects of material composition are examined using Spheral simulations (Figure 3, Table 1), while the sensitivity of  $\beta$  due to mechanical properties such as porosity are examined using both Spheral and CTH (Figures 3-5, Tables 1 and 2). These simulations used a range of compositions from granite to basalt and indicate that the

composition of the material has little effect on the momentum enhancement factor (Table 1). Porosity affects the momentum transfer more significantly, which is shown in both Spheral (Figure 3) and CTH simulations (Figure 4, 5). As porosity increases,  $\beta$  decreases. However, the actual imparted velocity ( $\Delta v$ ) to the material *increases*. The lower density results in a lower mass, which receives a correspondingly larger deflection for a given impulse.

The effect of porosity on the impact response was examined using CTH for multiple scenarios. Figure 4 shows the effect of increasing porosity on the crater formation and ejecta response for an impact of a basalt sphere into a basalt half-space. In general, as porosity increases the crater becomes increasingly narrow and deep, and the shape of the subsurface damage zone is altered. The ejecta is launched at higher angles for increasingly high porosities. Figure 5 showcases the effects of micro- and macro-porosity. A microporous target results in a slightly deeper and narrower crater than a coherent target. When an equivalent amount of macroporosity is included in the target instead, the crater is much larger, resulting in an increase of ejecta. Here, both  $\Delta v$  and  $\beta$  increase for a rubble-pile target compared to fully competent or microporous targets.

Table 1. Results from Spheral calculations for material with various compositions

Material	Porosity	Strength	Density g/cm <sup>3</sup>	$\Delta v$ (cm/s)	$\beta$
Granite	0.2	1 MPa	2.16	0.099	1.353
Basalt	0.2	1 MPa	2.16	0.102	1.391
Pumice	0.2	1 MPa	2.16	0.093	1.277
Granite	0.4	1 MPa	1.62	0.126	1.288

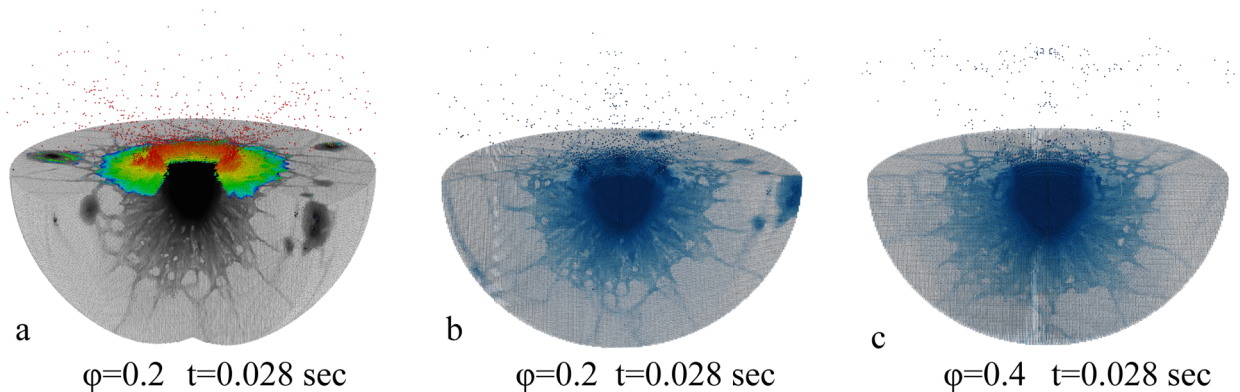


Figure 3. Spheral simulations of a 400-kg aluminum box impacting into a granite half-space at 7 km/s. Each simulation shows a region extending 13 m from the impact point. (a) Crater formation into a granite target 0.028 seconds after impact. The colors show the magnitude of the vertical velocity for material traveling at  $v > 5$  cm/s, while the gray values show the strain tensor trace. Quadrant is cut away to visualize interior. (b,c) Strain tensor trace in granite targets with 20% (b) and 40% (c) porosity. Half of domain is cut away to visualize interiors.

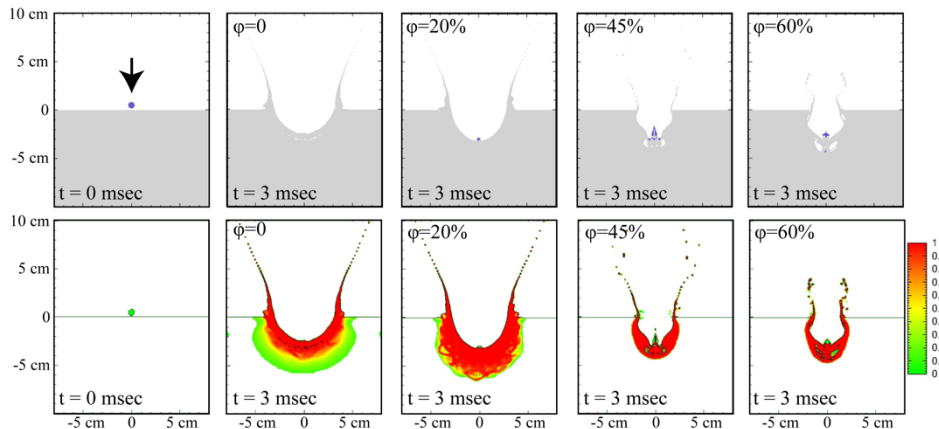


Figure 4. CTH simulations of a basalt sphere impacting into a basalt substrate at a variety of porosities. As porosity increases, beta will tend to decrease and the crater will become deeper and narrower.

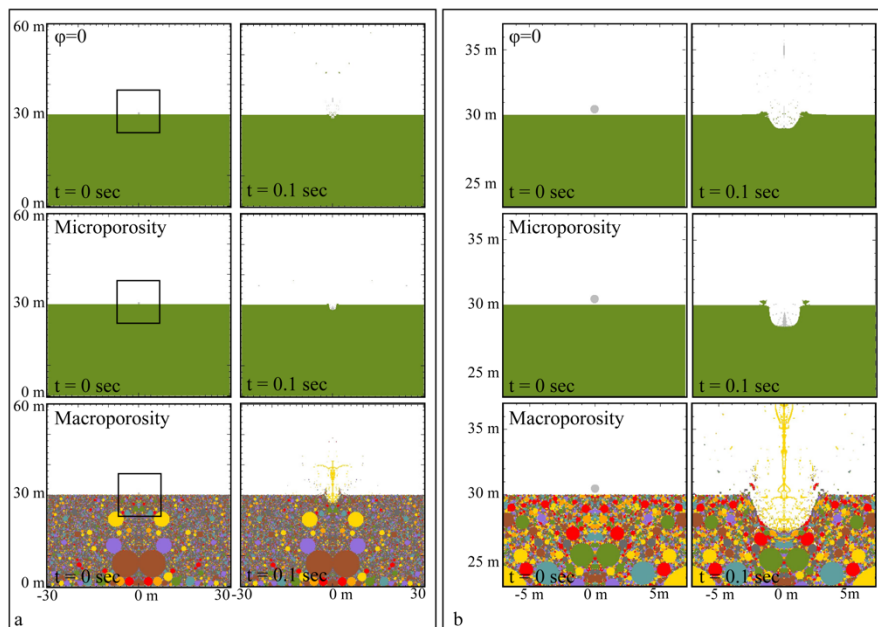


Figure 5. CTH simulations of a 30-cm aluminum sphere impacting into a basalt substrate at a variety of porosities. a) Initial setup and crater formation 0.1 sec after impact for a coherent target (top), a target with 20% microporosity (middle) and a target with 20% macroporosity (bottom). The black box shows the region highlighted in (b). The high ejecta plume in the center is a center-line effect in the 2D simulation.

Table 2. CTH simulations examining sensitivity of  $\beta$  to type of porosity

Projectile	Target	Porosity (%)	Impact velocity	$\beta$	$\Delta v$ (cm/s)	Reference Figure
60-cm aluminum sphere	basalt half space	0	6.25 km/s	1.32	1.75	Figure 5
	basalt half space, micro porous	~20	6.25 km/s	1.14	1.87	
	basalt half space, rubble pile	~20	6.25 km/s	1.55	2.53	



#### 4. Conclusions

Impact simulations in support of the Double Asteroid Redirection Test (DART) mission concept are used to place constraints on the possible outcomes of the DART impact into the moon of the 65803 Didymos system. While the spacecraft properties are well known, the target properties are largely unknown, requiring a large number of numerical simulations to fully understand the kinetic impact experiment and provide a means to extrapolate to other possible planetary defense scenarios. Here, material composition and strength properties were examined to determine the sensitivity of the momentum enhancement factor,  $\beta$ . Impact simulations into multiple compositions suggest that chemical composition should have little effect on the momentum enhancement from a kinetic impactor. Porosity of the material, however, has a large effect on the impact process: changing the crater shape, the ejecta flow field, the velocity imparted to the body, and the momentum enhancement from the impact. Increasing micro-porosity leads to a decrease in crater size and  $\beta$ , but an increase in  $\Delta v$ . If the target is represented as a “rubble pile” with significant macro-porosity, on the other hand, the crater size and  $\Delta v$  increase. Depending on how the projectile hits the target (either on a hard boulder or in between), macro-porosity can result in either an increase or a decrease in  $\beta$ . These sorts of impact simulations will provide our best means of interpreting the results of the DART impact, and ongoing work is examining the variety of possible impact scenarios and how they may affect  $\beta$ .

#### Acknowledgements

This study was funded by the NASA Double Asteroid Redirection Test. Parts of this work were performed under the auspices of the U.S. Department of Energy by Lawrence Livermore National Laboratory under Contract DE-AC52-07NA27344. LLNL-JRNL-731017.

#### References

- [1] Cheng, A. F., Atchison, J., Kantsiper, B., Rivkin, A. S., Stickle, A., Reed, C., et al. (2015). Asteroid impact and deflection assessment mission. *Acta Astronautica*, 115, 262–269.
- [2] Holsapple, K. A. (1993). The scaling of impact processes in planetary sciences, *Annual Review of Earth and Planetary Sciences*, 21, 333–373.
- [3] McGlaun, J.M., S.L. Thompson, and M.G. Elrick (1990). CTH: A three-dimensional shock wave physics code. *Int. J. Imp. Engr.* 10(1-4), 351–360.
- [4] Owen, J. M., Villumsen, J. V., Shapiro, P. R., & Martel, H. (1998). Adaptive smoothed particle hydrodynamics: Methodology. II. *The Astrophysical Journal Supplement Series*, 116(2), 155.
- [5] Owen, J. M. (2014). A compatibly differenced total energy conserving form of SPH. *International Journal for Numerical Methods in Fluids*, 75(11), 749–774.
- [6] Stickle, A.M. et al. (2016) Impact Simulation Benchmarking for the Double Asteroid Redirect Test (DART). *Proceedings of the 47<sup>th</sup> Lunar and Planetary Science Conference*, Abstract #2832.
- [7] Crawford, D.A. et al. 2006. Adaptive Mesh Refinement in the CTH Shock Physics Hydrocode, *The Russian Journal of Physical Chemistry B*, 25:9, p. 85–90.
- [8] Johnson, G.R., Cook, W.H., 1985. Fracture characteristics of three metals subjected to various strains, strain rates, temperatures and pressures. *Eng. Fract. Mech.* 21, 31–48.
- [9] Benz, W. and E. Asphaug (1999) Catastrophic Disruptions Revisited, *Icarus* 142, 5–20
- [10] Jutzi, M., Benz, W., and Michel P., 2008. Numerical simulations of impacts involving porous bodies I. Implementing sub-resolution porosity in a 3D SPH hydrocode, *Icarus*, p. 242–255.
- [11] Crawford, D.A. and Schultz, P.H. (2013) A model of localized shear heating with implications for the morphology and paleomagnetism of complex craters. *Large Meteorite Impacts Planet. Evol. V* 047.
- [12] Schultz, P.H. and D.A. Crawford (2016) Origin and implications of non-radial Imbrium Sculpture on the Moon, *Nature*, 535(7612), 391–394
- [13] Friedman, G. (2013) ParticlePack Users' Manual V3.0, Lawrence Livermore National Laboratory, LLNL-SM-649196.
- [14] Grady, D. E., & Kipp, M. E. (1980). Continuum modelling of explosive fracture in oil shale. In *International Journal of Rock Mechanics and Mining Sciences & Geomechanics Abstracts* (Vol. 17, No. 3, pp. 147–157)
- [15] Benz, W., & Asphaug, E. (1995). Simulations of brittle solids using smooth particle hydrodynamics. *Computer physics communications*, 87(1-2), 253–265.
- [16] Owen, J. M. (2010). ASPH modeling of Material Damage and Failure. Presented at the Proceedings of the 5th International SPHERIC Workshop, Manchester, UK.
- [17] Wünnemann, K., Collins, G. S., & Melosh, H. J. (2006). A strain-based porosity model for use in hydrocode simulations of impacts and implications for transient crater growth in porous targets. *Icarus*, 180(2), 514–527.
- [18] Asphaug, E., Ryan, E.V., and Zuber, M.T. (2002). Asteroid interiors. *Asteroids III*, 1, 463–484.
- [19] Jutzi, Martin, et al. "Numerical simulations of impacts involving porous bodies: II. Comparison with laboratory experiments." *Icarus* 201.2 (2009): 802–813.
- [20] Stickle, A.M. et al. (2015) Modeling Momentum Transfer from Kinetic Impacts: Implications for Redirecting Asteroids, *Procedia Engineering*, 103, 577–584.